Proceedings of ICRC 2001: 2348 © Copernicus Gesellschaft 2001

ICRC 2001

# Search for point sources and diffuse emission from the Galactic plane with the HEGRA-IACT-system

**H. Lampeitl[1], K. Bernlöhr[1], A. Daum[1], W. Hofmann[1], A. Konopelko[1], G. Pühlhofer[1], and HEGRA-Collaboration**

[1]Max Planck Institut für Kernphysik, Postfach 103980, D-69029 Heidelberg

**Abstract.** The HEGRA-IACT-system with a FoV of $\sim 1.5$ deg radius has been used for surveying one quater of the Galactic disc in respect to point sources, moderately extended sources and for diffuse emission in the energy range above 1 TeV. In total 140 h of good observation time were accumulated. No new source has been discoverd. Limits on the level of 20% or lower of the Crab flux on about 87 potential sources like SNR, Pulsars and EGRET sources are derived. A limit on the diffuse emission is given on the level of $d\Phi/dE$(E= 1 TeV) = $6.1 \cdot 10^{-15}$ ph cm$^{-2}$ s$^{-1}$ sr$^{-1}$ Mev$^{-1}$ resulting in a lower limit of 2.5 on the spectral index for the extrapolation of the meassured EGRET flux for the diffuse emission.

## 1 Introduction

Systems of imaging atmospheric Cherenkov telescopes, such as the HEGRA stereoscopic telescope system (Daum et al. 1997, Konopelko et al. 1999), allow to reconstruct the directions of air showers over the full field of view, with a radius of about 1.5°, and can therefore be used for sky surveys. Here, we report on two surveys, one along the galactic equator (GLP, Fig. 1) with the focus on the search for point sources and a second one perpendicular to the galactic equator (GLS, Fig. 2) with the focus on diffuse emission. The GLP scan, covering one quarter of the Galactic disk, from the galactic center to the Cygnus region, includes 105 h of observation time and is described in detail in Pühlhofer et al., 1999. Here we give results on individual point sources.
The second scan (GLS) covers a rectangular patch of the sky of roughly 80 deg$^2$, centered on the Galactic plane at longitude $40^\circ$ and includes 42 h of observation. The motivation for this survey was mainly the search for diffuse gamma-ray emission from the Galactic plane.
Diffuse emission results from the interactions of charged cosmic rays with interstellar gas confined to the plane or with photons. Diffuse emission in the energy range from tens of MeV to tens of GeV has been studied recently by EGRET (Hunter et al. 1997). The basic features can be modeled assuming $\pi^o$ decay as the dominant mechanism, with the gamma-ray emission proportional to the product of the gas column density and the cosmic-ray density (see, e.g., Hunter et al. 1997). Above 1 GeV, data show an excess in gamma-ray flux over model predictions (Hunter et al. 1997; see however Aharonian and Atoyan 2000). At these energies, contributions from inverse Compton scattering of electrons start to become relevant (see, e.g., Porter & Protheroe 1997). In response, revised models speculate that the local measurements of the electron flux may not be representative for the entire Galaxy (Porter & Protheroe 1997; Pohl & Esposito 1998). In case that the solar system is in an "electron void", diffuse gamma-ray emission at high energies could be an order of magnitude above predictions based on local electron spectra (Pohl & Esposito 1998). Another 'diffuse' gamma-ray flux component arises from the hard energy spectrum of those Galactic CRs that are still confined in the ensemble of their unresolved sources like SNRs (Berezhko & Völk, 2000).
The Galactic plane is also a region rich in potential gamma-ray point sources like SNRs as well as pulsar driven nebulae and unidentified EGRET sources. Theoretical models predict that typical gamma-ray fluxes from the majority of these objects are below the detection threshold of the current generation of instruments (see, e.g., Aharonian et al. 1997; Drury et al. 1994). However, both the lack of knowledge of the individual source parameters as well as approximations used in the modeling result in large uncertainties in the predictions for individual objects, by an order of magnitude or more.

## 2 Point Sources

Point sources were searched in both scans on a grid where the bin position is taken to be the source position. A grid

*Correspondence to:* H. Lampeitl
(lampeitl@daniel.mpi-hd.mpg.de)

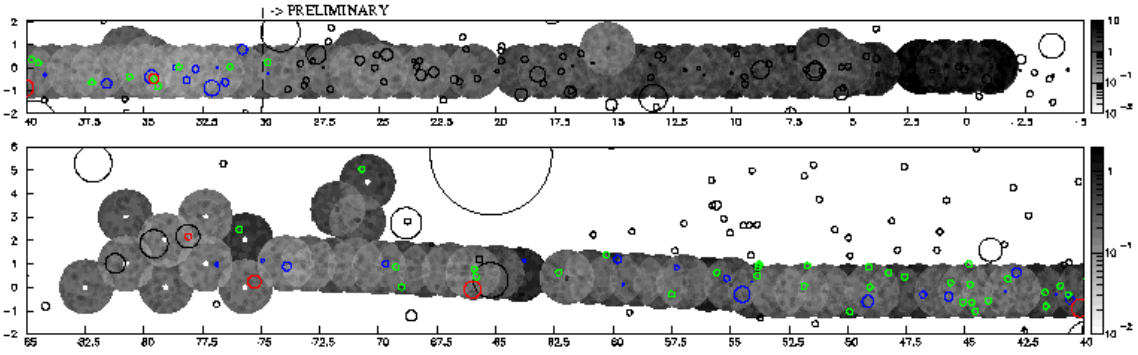


**Fig. 1.** Galactic Longitude Scan (GLP). Derived upper limits for point sources in units of the flux from the Crab Nebula. Circles indicate positions of potential TeV-gamma-ray emitters like Pulsars, SNR and EGRET GeV sources.

| Pulsar | $\sigma$ | [CU] | Pulsar | $\sigma$ | [CU] |
|---|---|---|---|---|---|
| J1844-0244 | -1.0 | 0.28 | J1914+1122 | 0.8 | 0.23 |
| J1848-0123 | 2.2 | 0.43 | J1915+07[b] | -1.1 | 0.22 |
| J1852+00 | -0.3 | 0.14 | J1915+1009 | -0.7 | 0.14 |
| J1854+10[b] | -0.8 | 0.29 | J1916+1030 | -1.7 | 0.1 |
| J1856+0113 | -0.6 | 0.15 | J1916+0951 | 0.2 | 0.18 |
| J1857+0057 | -0.8 | 0.13 | J1916+1312 | 1.0 | 0.34 |
| J1857+0212 | -1.3 | 0.14 | J1917+1353 | 2.1 | 0.34 |
| J1901+0331 | -0.9 | 0.18 | J1918+1444 | 0.4 | 0.32 |
| J1901+0716[b] | 0.2 | 0.11 | J1921+1419 | 1.1 | 0.19 |
| J1902+0556[b] | 0.5 | 0.06 | J1923+17 | -0.6 | 0.24 |
| J1902+06[b] | -0.3 | 0.06 | J1926+1648 | -0.2 | 0.13 |
| J1902+07[b] | 0.7 | 0.08 | J1926+1434 | 0.3 | 0.38 |
| J1904+10[b] | 0 | 0.53 | J1927+1855 | 0 | 0.87 |
| J1905+0709[b] | -0.2 | 0.08 | J1927+1856 | -0.5 | 0.36 |
| J1906+0641[b] | -0.5 | 0.05 | J1929+18 | -0.7 | 0.13 |
| J1908+07[b] | -0.7 | 0.07 | J1932+2020 | -1.1 | 0.18 |
| J1908+0916 | 0.1 | 0.16 | J1939+24 | -0.3 | 0.21 |
| J1908+04[b] | -2.4 | 0.05 | J1939+2134 | 0.6 | 0.17 |
| J1908+0916[b] | 2.4 | 0.32 | J1946+26 | 0.4 | 0.19 |
| J1909+1102 | -1.1 | 0.36 | J1948+3540 | 1.7 | 0.56 |
| J1909+0254[b] | -1.1 | 0.15 | J1954+2923 | 0.3 | 0.13 |
| J1910+0358[b] | -0.7 | 0.09 | J1955+2908 | -1.8 | 0.08 |
| J1910+07[b] | 0 | 0.09 | J2002+3217 | -1.5 | 0.11 |
| J1912+10 | 1.0 | 0.24 | J2004+3137 | -0.4 | 0.29 |
| J1913+09 | -1.5 | 0.09 | J2013+3845 | 0.4 | 0.46 |

| SNR | $\sigma$ | [CU] | SNR | $\sigma$ | [CU] |
|---|---|---|---|---|---|
| G29.7-0.3 | -0.7 | 0.28 | G45.7-0.4[3] | -1.7 | 0.15 |
| G30.7+1.0[3] | -0.4 | 0.46 | G46.8-0.3[2] | 1.0 | 0.35 |
| G31.5-0.6[2] | -0.9 | 0.19 | G49.2-0.7[3] | -0.5 | 0.21 |
| G31.9+0.0[1] | 0.1 | 0.1 | G54.1+0.3 | -0.3 | 0.17 |
| G32.1-0.9[4] | 0.8 | 0.6 | G54.4-0.3[4] | -0.6 | 0.27 |
| G32.8-0.1[2] | 1.1 | 0.45 | G55.0+0.3[2] | -0.1 | 0.21 |
| G33.2-0.6[2] | 1.4 | 0.25 | G57.2+0.8[1] | 0.3 | 0.11 |
| G33.6+0.1[1] | 0.4 | 0.15 | G59.5+0.1[1] | 1.4 | 0.26 |
| G34.7-0.4[4] | -0.7 | 0.3 | G59.8+1.2[2] | 0.6 | 0.4 |
| G36.6-0.7[3] | 1.1 | 0.45 | G63.7+1.1[1] | 0 | 0.35 |
| G39.2-0.3[b] | 1.04 | 0.08 | G69.7+1.0[2] | 0.2 | 0.17 |
| G40.5-0.5[2b] | -0.9 | 0.06 | G73.9+0.9[3] | 0 | 0.18 |
| G41.1-0.3[b] | 1.0 | 0.1 | G74.9+1.2[1] | 0.8 | 0.15 |
| G42.8+0.6[2b] | 1.1 | 0.26 | G76.9+1.0[1] | 0.4 | 0.13 |
| G43.3-0.2 | -0.7 | 0.14 | | | |
| GeV | | | | | |
| J1856+0115[3] | -2.7 | 0.11 | J2020+3658[4] | 0.4 | 0.27 |
| J1907+0557[5] | -0.3 | 0.78 | J2020+4023[2] | 0 | 0.15 |
| J1957+2859[5] | -2.3 | 0.2 | | | |

**Table 1.** Significances and upper limits in units of the Crab flux (CU). (b): Limit derived from GLS-Scan. Source bin radius:(1) $\vartheta = 0.18^o$, (2) $\vartheta = 0.2^o$, (3) $\vartheta = 0.25^o$, $\vartheta = 0.3^o$, (4) $\vartheta = 0.4^o$, (5) $\vartheta = 0.5^o$. Source positions and sizes taken from Tayler et al. 1993, Green 1998, Lamb et al. 1997. Limits on W50 will be reported in Rowell G., 2001

spacing below the angular resolution of $\approx 0.1^o$ is chosen of $0.0625^o$ in case of the GLS-scan and of $0.03125^o$ in case of the GLP-scan. The radius of the source bin for point sources is chosen according the angular resolution of the telescope configuration to optimize $S/\sqrt{B}$. In case of moderately extendet objects the radius of the source bin was adapted such, that the complete source fits in the search bin. To estimate backgrounds, three regions of the same size as the source region were used, rotated by 90°, 180° and 270° around the telescope axis, relative to the source. Significances for a detection are then calculated according to Li & Ma (1983). Since no high significant source bin is found in both scans upper limits are calculated using the procedure of O. Helene (1983). To convert from counts to fluxes in the case of the GLP-scan Crab data are used for calibration, in case of the GLS-scan the expected number of counts are derivied from MC simulations. The simulations show that the result on the differential flux upper limit depends only weak on the spectral index at 1 TeV (see Aharonian et al., 1995).

Fig. 1 shows a map of resulting upper limits for point sources for the GLP-scan. Analysis is carried out for sources with $l > 30^o$ corresponding to zenith angels $< 30^o$ and results on individual sources are given in Tab. 1. Results on smaller galactic longitude are preliminary and no individual upper limits are given. For the GLS-scan results are shown in Fig.

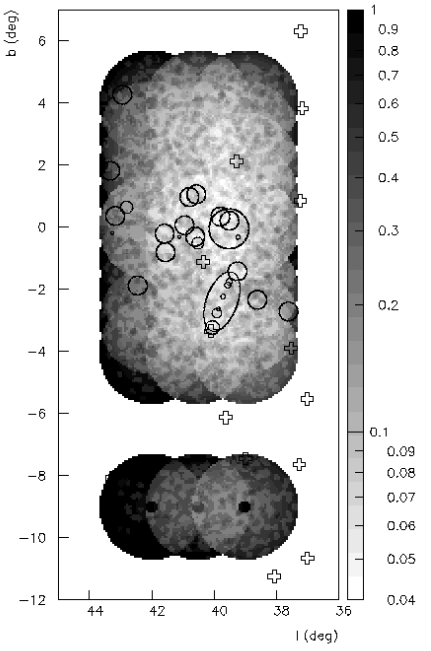


**Fig. 2.** Galactic Latitude Scan (GLS). Derived upper limits for point sources in units of the flux from the Crab Nebula.

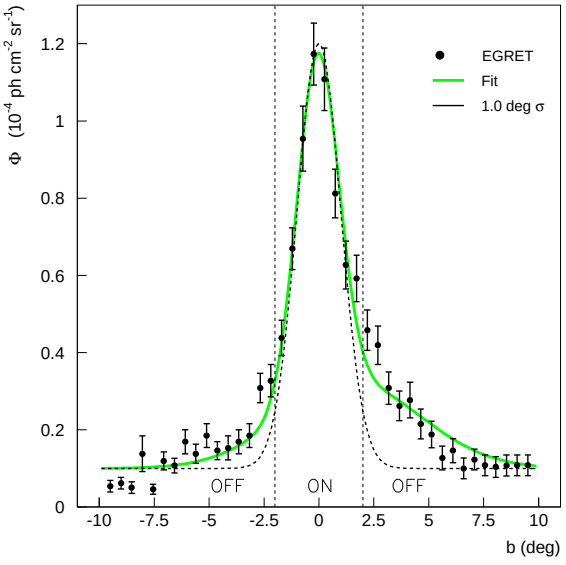


**Fig. 3.** Latitude dependence of the diffuse emission measured by EGRET for photon energies above 1 GeV, in the range of Galactic longitude 30° to 50°, together with a fit by a sum of two Gaussians. Data points taken from Hunter et al. 1997. In addition a Gaussian profiles with a $\sigma$ of $1.0°$, is shown.

2 and in Tab. 1.

## 3 Diffuse Emission

The search for diffuse gamma-ray emission from the Galactic plane is complicated by the extended structure of the emission region. The structure may be extended in latitude beyond the field of view. Fig. 3 illustrates the profile in Galactic latitude as measured by EGRET.

To achive low threshold, observations were carried out under small zenith angles ($z < 30^o$) in June, July and August 1999. Emphasis was on the control of systematic effects like changing weather conditions.

The most robust and model-independent – but also least sensitive – technique to derive limits on the diffuse flux simply selects 5-telescope-events according to their shapes as gamma-ray candidates. A cut on $\bar{w}$ less than 1.0 keeps about 1/2 of the gamma-rays, but rejects cosmic rays very efficiently. Assigning all 428 events after cuts as diffuse gamma-rays a 99% upper limit on the diffuse gamma-ray flux at 1 TeV of 23.4 $\cdot 10^{-15}$ ph cm$^{-2}$ s$^{-1}$ sr$^{-1}$ MeV$^{-1}$ results, for $|b| < 5°$, assuming a flux from the Crab nebula of $2.7 \cdot 10^{-17}$ ph cm$^{-2}$ s$^{-1}$ MeV$^{-1}$ at 1 TeV (Aharonian et al., 2000).

The limit obtained by this technique can be improved by subtracting, on a statistical basis the background, using an experimental background region, sufficiently far away from the Galactic plane. Data sets can be normalized to each other using the rates of events with large $\bar{w}$ ($> 1.4$), well outside the gamma-ray region. Unfortunately, the availability of suitable background data samples with the same telescope configuration is limited to 4.1 h of data, limiting the sensitivity. After a $\bar{w} < 1.1$ cut 1928 events survived compared to 141 events in the reference sample. After subtraction of isotropic components, we find a 99% limit on the diffuse flux in the region $|b| < 5°$ of 10.4 $\cdot 10^{-15}$ ph cm$^{-2}$ s$^{-1}$ sr$^{-1}$ MeV$^{-1}$ at 1 TeV.

The final, and most sensitive analysis makes the assumption that diffuse gamma-ray emission from the Galactic plane is limited to the central parts of the scan region, and uses the outer parts of the scan region to estimate backgrounds. The signal region was considered $|b| < 2°$. To ensure optimum quality of the events, only four- and five-telescope events were used, and the field of view was restricted to 1.5° from the optical axis. A cut at 1.1 on the $\bar{w}$ was applied to reject cosmic-ray background. To account for a possible zenith-angle dependence of background rates, data were grouped into four different ranges in zenith angle, 20°-24°, 24°-28°, 28°-32° and 32°-36°. For each range in zenith angle and each scan band, the expected number of events in the signal region was calculated based on the number of events observed in the corresponding areas of the camera for the background region. The expected and observed numbers of events were then added up for all zenith angles and scan bands. With a total number of 2387 gamma-ray events in the signal region, compared to 2353 expected events, there is no significant excess (see Fig. 4).

In order to translate the limit in the number of events into a flux limit, one now has to make assumptions concerning the distribution in Galactic latitude of the diffuse radiation, since

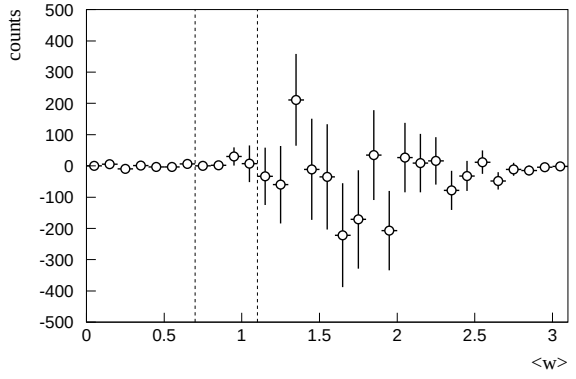


**Fig. 4.** Difference between the distributions in mean scaled width for the on-region ($|b| < 2^\circ$) and for the off-region ($|b| > 2^\circ$). The dashed lines indicate the expected gamma-ray region.

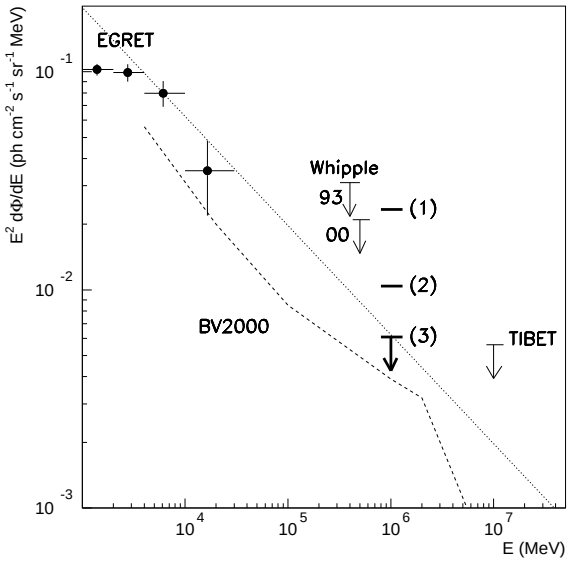


**Fig. 5.** Upper limits for the diffuse gamma-ray flux derived by this experiment. Assuming that all detected events are gamma-rays (1), using a independent data set for background subtraction (2), and using $|b| > 2^\circ$ as background data and assuming the spatial distribution measured by the ERGRET instrument ($38^\circ < l < 43^\circ, |b| < 2^\circ$) (3). For detailed explanations see text. Also shown is the EGRET flux for $35^\circ < l < 45^\circ, |b| < 2^\circ$, the Whipple upper limits for $38.5 < l < 41.5^\circ, |b| < 2^\circ$ (Reynolds et al. 1993, LeBohec 2000) and the Tibet upper limit (Amenomori, 1997). The dotted line indicates an extrapolation of the EGRET data with an index of 2.5. The dashed line indicates the scaled 'leaky box' model prediction by Berezhko & Völk, 2000 (BV2000).

a spill-over of diffuse gamma-rays into the background region $|b| > 2^\circ$ will effectively reduce the signal. For a profile with a width less or comparable to the EGRET profile a correction of 12% is applied and one finds a limit $6.1 \cdot 10^{-15}$ ph cm$^{-2}$ s$^{-1}$ sr$^{-1}$ MeV$^{-1}$ for the diffuse gamma-ray flux at 1 TeV, averaged over the $|b| < 2^\circ$ region. The limit refers to an assumed spectral index of -2.6, and changes by +13% for an index of -2, and by -5% for an index of -3. For wider distributions of $2^\circ$ and $3^\circ$ rms, the limit changes to $8.2 \cdot 10^{-15}$ ph cm$^{-2}$ s$^{-1}$ sr$^{-1}$ MeV$^{-1}$ and $12.8 \cdot 10^{-15}$ ph cm$^{-2}$ s$^{-1}$ sr$^{-1}$ MeV$^{-1}$, respectively. Results are summarized in Fig. 5.

## 4 Concluding remarks

No strong TeV-gamma-ray emitter is detected in roughly one quater of the Galactic disc coverd by both scans. Limits derived for known sources are on the level or lower than 20% of the Crab flux.

A search for diffuse gamma-ray emission resulted in an upper limit of $6.1 \cdot 10^{-15}$ ph cm$^{-2}$ s$^{-1}$ sr$^{-1}$ MeV$^{-1}$ at 1 TeV averaged over the region $38^\circ < l < 43^\circ, |b| < 2^\circ$ and assuming the spatial emission profile measured by the EGRET instrument. Since the analysis used to derive this limit is only sensitive to the variation of the diffuse flux with $b$, rather than its absolute value, a distribution significantly wider than at EGRET energies will increase the limit. Other variants of the data analysis are sensitive to the absolute flux, but give less stringent limits of 23.4 and $10.4 \cdot 10^{-15}$ ph cm$^{-2}$ s$^{-1}$ sr$^{-1}$ MeV$^{-1}$. The limit on the TeV gamma-ray flux can be used to derive a lower limit on the spectral index of the diffuse radiation of 2.5, and to exclude models which predict a strong enhancement of the diffuse flux.

*Acknowledgements.* The support of the HEGRA experiment by the German Ministry for Research and Technology BMBF and by the Spanish Research Council CYCIT is acknowledged.

## References

Aharonian et al., 1995, J. Phys. G 21, 419
Aharonian, F. et al., 1997, MNRAS 291, 162
Aharonian et al., 2000, ApJ, 539, 317
Aharonian, F. A. & Atoyan, A. M. 2000, A&A, 362, 937
Amenomori, M. et al., 1997, Proc. 25th ICRC, Durban, 3, 117
Berezhko, E.G, Völk, H.J., 2000, ApJ 540, 923
Borione, A., et al., 1997, ApJ 493, 175
Daum, A., et al., 1997, Astropart. Phys. 8, 1
Drury, L.O. et al.,1994, A&A, 287, 959
Rowell, G., 2001, this proceedings
Green, D.A.,Mullard Radio Astronomy Observatory, 1998
Helene, O., 1983, NIM 212, 319
Hunter et al., 1997, ApJ 481, 205
Konopelko, A., et al., 1999, Astropart. Phys., 10, 275
Lamb R.C., Macomb D.J., 1997, ApJ, 488, 872
LeBohec, S., et al., 2000, ApJ 539, 209
Li, T., Ma, Y., 1983, ApJ 272, 317
Pohl, M., Esposito, J.A., 1998, ApJ 507, 327
Porter, T.A., Protheroe, R.J., 1997, J. Phys. G 23, 1765
Pühlhofer, G, et al. 1999, Proc. 26th ICRC, 77
Reynolds, P.T. et al., 1993, ApJ 404, 206
Tayler, J.H. et al., 1993, ApJSS 88, 529